

Partition Generative Modeling: Masked Modeling Without Masks

Justin Deschenaux^{1*}Lan Tran¹Caglar Gulcehre¹¹EPFL, Lausanne, Switzerland

Abstract

We introduce “Partition Generative Models” (PGMs), a novel approach to masked generative modeling (MGMs), particularly effective for masked diffusion language modeling (MDLMs). PGM divides tokens into two distinct groups and employs sparse attention patterns to prevent cross-group information exchange. Hence, the model is trained to predict tokens in one group based solely on information from the other group. This partitioning strategy eliminates the need for MASK tokens entirely. While traditional MGMs inefficiently process MASK tokens during generation, PGMs achieve greater computational efficiency by operating exclusively on unmasked tokens. Our experiments on OpenWebText with a context length of 1024 tokens demonstrate that PGMs deliver at least 5x improvements in both latency and throughput compared to MDLM when using the same number of sampling steps, while generating samples with better generative perplexity than MDLM. Finally, we show that PGMs can be distilled with Self-Distillation Through Time (SDTT), a method originally devised for MDLM, in order to achieve further inference gains.

1 Introduction

Masked generative modeling (MGM) excels at sampling from complex data distributions by iteratively denoising masked inputs. In fact, the MGM paradigm has proven successful in various modalities, such as images [8], video [54, 49], and audio spectrograms [11]. In particular, recent advances leveraging discrete diffusion [6, 56, 27, 36, 41, 30] and discrete flow matching [7, 17] have shown that MGM can also be applied to text generation, challenging the traditional dominance of autoregressive modeling in this domain.

Modern MGMs use the transformer architecture [48] with bidirectional attention to reconstruct masked tokens. This simple approach, which can be seen as a form of generalized BERT [13] model, can generate new samples by iteratively denoising a sequence of masked inputs.

Despite their ability to generate high-quality samples, MGMs face two key inference effi-

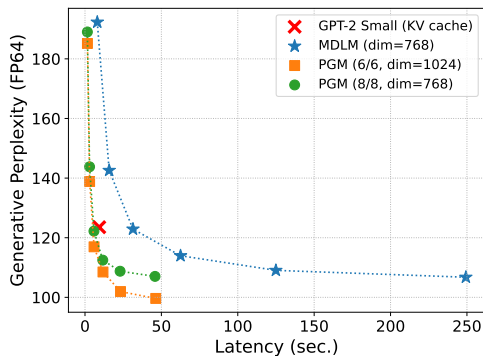


Figure 1: **Latency results:** PGM (ours) achieves better *generative perplexity* and at least 5x improvements in latency compared to MDLM on OpenWebText [18]. Samples are generated using power-of-2 step counts with 32 to 1024 steps. The latency improvements come from our specialized neural network architecture.

*Correspondence to justin.deschenaux@epfl.ch.

ciency challenges compared to autoregressive models (ARM). Firstly, unlike ARMs, which benefit from KV caching [34], MGM transformers must recompute all activations in each decoding step. Secondly, MGMs process many masked tokens that carry minimal information, particularly in the early sampling stages, when most tokens are masked. In contrast, ARMs only need to process tokens they have already generated.

In this work, we introduce ‘‘Partition Generative Models’’ (PGM). This novel approach does not require processing masked tokens during training and inference and can be implemented using simple attention masking. The key insight behind PGM is simple: during training, instead of masking tokens, we partition them into two disjoint groups and train the model to predict one group from the other. As shown in Figure 2 (right), PGMs only process unmasked tokens during sampling. In contrast, MGMs must always handle full-length sequences. This leads to a significant performance gain for PGMs. Furthermore, while most MGMs compute predictions for all missing positions, PGMs can produce logits solely for the positions that will be effectively denoised in the current sampling step.

Our main contributions can be summarized as follows.

- We introduce ‘‘Partition Generative Models’’ (PGM), a simple and effective alternative to Masked Generative Modeling (MGM). We propose an encoder-decoder variant of the diffusion transformer [33] that does not need to process any masked token at inference.
- PGM achieves a reduction of 1.95 in perplexity in LM1B [9], compared to masked diffusion language models (MDLM) [36]. In OpenWebText [18], PGMs can generate samples of better quality than MDLM with a 5- 5.5x improvement in throughput and latency, when using the same number of sampling steps as MDLM.
- Additionally, we show that PGMs can be distilled [12] and achieve 10.73x better latency and superior generative perplexity than GPT-2 with KV caching.

2 Background

2.1 Generative Language Modeling

Language modeling addresses the task of generating sequences of discrete tokens (x_i) from a vocabulary $\mathcal{X} = \mathbb{Z}^{<N} = \{0, \dots, N - 1\}$. A language model generates sequences of length L , defined as elements of $\mathcal{X}^L = \left\{ \mathbf{x}^{(i)} = (x_0^{(i)}, \dots, x_{L-1}^{(i)}) : x_j^{(i)} \in \mathcal{X} \right\}_{i=0}^{N^L}$. The training data set $\mathcal{D} := \{ \mathbf{x}^{(0)}, \dots, \mathbf{x}^{(K-1)} : \mathbf{x}^{(i)} \in \mathcal{X}^L \}$ contains K such sequences. One fundamental objective of language modeling is to generate samples similar to those of the unknown distribution $p_0 : \mathcal{X}^L \rightarrow [0, 1]$ that induced the training data set \mathcal{D} .

2.2 Masked Generative Modeling

In MGM, the vocabulary \mathcal{X} includes a special MASK token absent from the training set \mathcal{D} . During training, the MASK token is used to replace a fraction of the original tokens in the input sequences $\mathbf{x} \in \mathcal{D}$. Formally, we train a denoiser $\mathbf{x}_\theta : \mathcal{X}^L \rightarrow \mathbb{R}^{L \times N}$ with learnable parameters θ . To generate new samples, we initialize the sampling procedure with sequences composed entirely of MASK tokens. The model then iteratively replaces a subset of these masked tokens according to a predefined algorithm, for example, denoising a random subset of the MASK tokens. The training objective of the denoiser \mathbf{x}_θ can generally be written as follows:

$$\mathcal{L}_{\text{MGM}} := \mathbb{E}_{\mathbf{x} \sim \mathcal{D}, t \sim \mathcal{U}[0,1]} [w(t) \text{CE}(\mathbf{x}_\theta(\mathbf{z}_t; t), \mathbf{x})], \quad (1)$$

where t determines the proportion of tokens to mask. The corrupted sequence \mathbf{z}_t is generated by independently masking each token in \mathbf{x} with time-dependent probability p_t . For simplicity, we could set $p_t = t$. The weighting function $w : [0, 1] \rightarrow \mathbb{R}_{\geq 0}$ allows us to assign a different importance to each noise level. Finally, $\text{CE}(x, y)$ denotes the cross-entropy loss between the predicted logits x and the target integer labels y . Oftentimes, the cross-entropy loss is applied exclusively to masked tokens. In such cases, the denoiser model \mathbf{x}_θ is implemented to assigns all probability mass to the input token at positions where the input tokens are *not* masked.

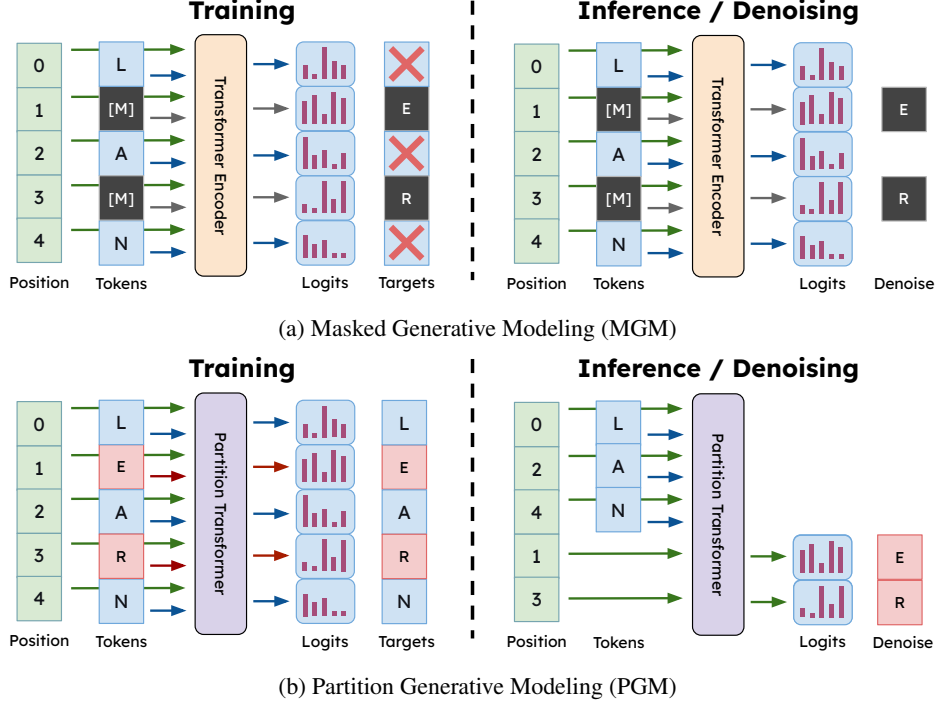


Figure 2: **Masked Generative Modeling (MGM) vs. Partition Generative Modeling (PGM).** **Training:** PGMs receive feedback at every position, while MGMs usually only apply loss to masked tokens. **Inference:** PGMs process only unmasked tokens, working with shorter sequences and predicting logits only for tokens to denoise. MGMs must process full-length sequences and compute logits at all positions. **Important note:** PGMs use a specialized architecture that ensures predictions for position i never depend on the token at position i .

2.3 Masked Diffusion Language Modeling

“Masked diffusion language models” (MDLM) are sequence generative models that operate in discrete space. MDLMs have demonstrated performance comparable to Autoregressive models in validation perplexity and text generation quality. In this work, we use MDLM as our baseline MGM implementation and focus our main experiments on text generation.

Discrete Absorbing Diffusion Process MDLMs define a forward process that corrupts the data and a backward process that recovers it. For each token in the sequence, the forward process linearly interpolates between the one-hot encoding of each token in \mathbf{x} and π , the absorbing distribution that assigns all mass to the MASK token. Formally:

$$q(\mathbf{z}_t|\mathbf{x}) := \text{Categorical}(\mathbf{z}_t; \alpha_t \mathbf{x} + (1 - \alpha_t) \pi), \quad (2)$$

where α_t defines the noise injection schedule for $t \in [0, 1]$. This schedule must be such that $\alpha_t \in [0, 1]$, α_t is strictly decreasing as t increases, and should satisfy the boundary conditions $\alpha_0 \approx 1$ and $\alpha_1 \approx 0$. The process is termed “absorbing” because the corruption is irreversible. Once a token becomes a MASK token, it remains masked throughout the forward process. The posterior sampling distribution $p_\theta(\mathbf{z}_s|\mathbf{z}_t)$ uses the same analytical form as the true posterior $p(\mathbf{z}_s|\mathbf{z}_t, \mathbf{x})$, where \mathbf{x} denotes a sample from the data distribution. Since \mathbf{x} is not available during sampling, the output of the denoiser \mathbf{x}_θ is used in place of \mathbf{x} . Formally, $p_\theta(\mathbf{z}_s|\mathbf{z}_t) := q(\mathbf{z}_s|\mathbf{z}_t, \mathbf{x} = \mathbf{x}_\theta(\mathbf{z}_t; t))$. To derive a simple expression for $p_\theta(\mathbf{z}_s|\mathbf{z}_t)$, MDLM enforces that unmasked tokens are carried over during reverse diffusion, which induces the following expression:

$$p_\theta(\mathbf{z}_s|\mathbf{z}_t) = \begin{cases} \text{Cat}(\mathbf{z}_s; \mathbf{z}_t), & \mathbf{z}_t \neq \mathbf{m}, \\ \text{Cat}\left(\mathbf{z}_s; \frac{(1-\alpha_s)\mathbf{m} + (\alpha_s - \alpha_t)\mathbf{x}_\theta(\mathbf{z}_t, t)}{(1-\alpha_t)}\right), & \mathbf{z}_t = \mathbf{m} \end{cases} \quad (3)$$

Training Objective MDLM trains the denoiser \mathbf{x}_θ using a continuous-time negative evidence lower bound (NELBO) [44], which provides a tighter bound to the log-likelihood of the data than the discrete-time NELBO [26]. The denoiser defines a learned posterior distribution $p_\theta(\mathbf{z}_s|\mathbf{z}_t) := q(\mathbf{z}_s|\mathbf{z}_t, \mathbf{x}_\theta(\mathbf{z}_t, t))$, and the NELBO simplifies to a weighted cross-entropy loss between ground-truth samples \mathbf{x} and the predictions of the denoiser \mathbf{x}_θ :

$$\mathcal{L}_{\text{NELBO}}^\infty = \mathbb{E}_q \int_{t=0}^{t=1} \frac{\alpha'_t}{1 - \alpha_t} \log \langle \mathbf{x}_\theta(\mathbf{z}_t, t), \mathbf{x} \rangle dt. \quad (4)$$

2.4 Self-Distillation Through Time

“Self-Distillation Through Time” (SDTT) [12] speeds up the sampling of MDLMs through a process similar to “Progressive Distillation” [39]. SDTT creates student and teacher copies from a pre-trained MDLM. The student learns to match the prediction that the teacher makes in two steps of size dt . After convergence, the student can be used for a new round of distillation with a step size of $2dt$, further decreasing the number of sampling steps by a factor of two.

3 Partition Generative Modeling

3.1 Motivations

“Partition Generative Modeling” (PGM) is based on MGM but introduces key modifications to the training and sampling procedures. Most notably, PGMs eliminate the need for MASK tokens.

Training As seen in Figure 2a (left), in a single forward pass of an MGM, a loss can be computed for the masked positions only. In contrast, autoregressive language (AR) models receive a training signal at every position in a single forward pass. Intuitively, this discrepancy could make MGMs less sample-efficient than AR models. We design PGMs such that we can compute the loss at every position in the sequence in a single forward pass, as shown in Figure 2b (left).

Sampling MGMs typically employ bidirectional architectures trained on fixed-length inputs. Consequently, during sampling, these models process arrays with the same dimensions as those used during training. Hence, during the initial sampling steps, the neural network processes primarily MASK tokens. These tokens provide minimal information, only indicating the current noise level. On the other hand, autoregressive models only process previously generated tokens. Additionally, MGMs compute predictions for all masked positions, whereas autoregressive models only generate predictions for the one position to denoise. PGMs only process previously generated tokens and compute predictions solely for tokens that will be denoised (Figure 2b, right). Hence, PGMs maintain the parallel decoding capabilities of MGMs while offering substantial inference speedups.

3.2 Approach

Partitioning Tokens Instead of Masking For a training sequence $\mathbf{x} \in \mathcal{D}$, we partition tokens into two distinct groups labeled 0 and 1, rather than using MASK tokens. From the perspective of each group, tokens in the other group will not be visible due to constraints on the neural network architecture, even though no explicit MASK token is used. Because each training sequence is partitioned into two groups that predict each other, PGMs implement a mechanism that creates two subtraining examples per “physical” sequence in the batch. Hence, a similar performance improvement could be expected *as if we were training an MGM with a twice larger batch size, with complementary masking between copies*. We isolate and study the effect of complementary masking from the neural architecture in Section 5.3.

Training Objective Let $\mathbf{g} \in \{0, 1\}^L$ be the binary sequence that denotes the group index of each token in \mathbf{x} . We train a denoiser network \mathbf{x}_θ that takes as input \mathbf{x} and \mathbf{g} , and we ensure that only tokens in the same group are involved with each other to avoid information leakage. From the objective, \mathbf{x}_θ is trained to predict its input, which is only useful because of the constraints on the attention:

$$\mathcal{L}_{\text{PGM}} := \mathbb{E}_{\mathbf{x} \sim \mathcal{D}, t \sim \mathcal{U}[0,1]} [w^{\text{PGM}}(\mathbf{g}, t) \text{CE}(\mathbf{x}_\theta(\mathbf{x}; \mathbf{g}; t), \mathbf{x})]. \quad (5)$$

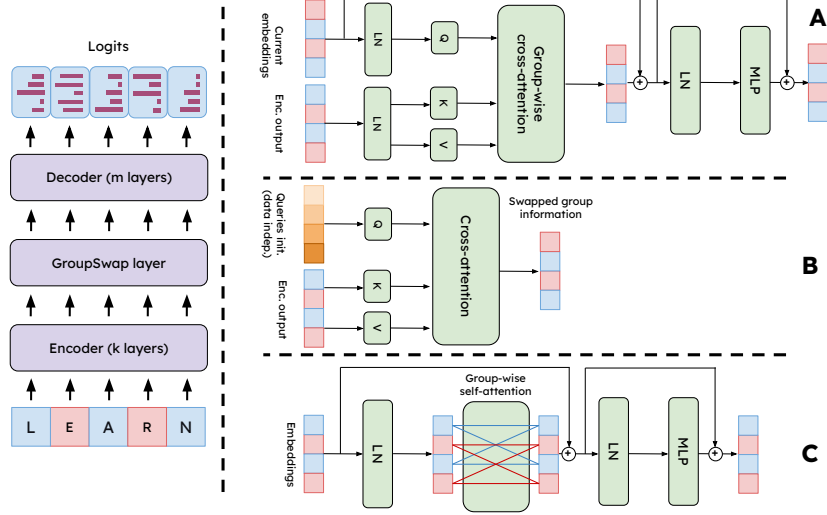


Figure 3: **PGM-compatible transformer architecture.** RoPE [46] is applied before every attention layer but not shown for clarity. (A) Decoder layer with cross-attention to the encoder output and no self-attention between tokens. (B) GroupSwap layer that exchanges information between positions in group 0 and group 1, enabling each group to make predictions based on tokens from the other group. (C) Encoder layer with sparse, group-wise self-attention.

The key distinction from Equation 1 lies in the weighting function w^{PGM} . Let $t \in [0, 1]$ be the probability of assigning a token to the group 1. Hence, the tokens in group 0 perceive a noise level of t , while those in group 1 perceive a noise level of $1 - t$. Therefore, we must scale the loss for tokens in group 0 according to the noise level t , and by $1 - t$ for tokens in group 1. Let w represent the weighing function used to train an MGM. Then, the corresponding weight function w^{PGM} to train PGMs is defined as

$$w^{\text{PGM}}(\mathbf{g}, t)_i = \begin{cases} w(t) & \text{if } \mathbf{g}_i = 0 \\ w(1 - t) & \text{if } \mathbf{g}_i = 1. \end{cases} \quad (6)$$

We adopt the weighting function of MDLM, namely $w(t) = \frac{\alpha_t'}{1 - \alpha_t'}$, defined in Equation 4. A visual comparison of the training processes for MGM and PGM is provided in Figure 2 (left).

Sampling Since PGMs are trained without communication between tokens in different partitions, PGMs can process only unmasked tokens (Figure 2b, right) during inference. Assuming the same posterior distribution $p_\theta(\mathbf{z}_s | \mathbf{z}_t)$ (Equation 3) as MDLM, an MGM denoises MASK tokens randomly and independently with probability $\frac{\alpha_s - \alpha_t}{1 - \alpha_t}$. When implemented as a PGM, it means that one can equivalently select a subset of tokens and compute predictions exclusively for those positions, which drastically improves the inference efficiency while retaining the parallel generation abilities. To simplify the implementation of batched sampling, PGM can denoise a fixed number of tokens at each sampling step, unlike MDLM, which denoises a random number of tokens. The pseudocode is presented in Algorithm 1. PGMs can also sample a random number of tokens at each step, though this requires padding batched sequences. We provide the pseudocode for this approach in Algorithm 2 and compare the perplexity, latency, and throughput of both approaches in Table 5.

4 PGM Compatible Transformer Architecture

Figure 3 illustrates our proposed PGM-compatible transformer model. The architecture consists of three components: an encoder, a GroupSwap layer, and a decoder.

Encoder The encoder consists of a series of partition-wise self-attention transformer blocks. These blocks operate like standard transformer blocks with bidirectional attention, with the key difference

Algorithm 1 Simplified Sampling for PGMs

```
1: Input: Batch size BS, number of steps K, model length L, special BOS index
2: Output: Generated samples x
3: x  $\leftarrow$  empty_tensor(BS, 1)  $\triangleright$  Initialize
4: x[:, 0]  $\leftarrow$  BOS  $\triangleright$  Set BOS as first token
5: k  $\leftarrow$  L/K  $\triangleright$  Number of tokens to denoise at each step
6: decoded_positions  $\leftarrow$  zeros(BS, 1)  $\triangleright$  Keep track of already-decoded and positions to decode
7: positions_to_decode  $\leftarrow$  1+ rand_row_perm(BS, L-1)  $\triangleright$  Each rows is a permutation of  $\{1, \dots, L\}$ 
8: for _ in range(K) do
9:   pos_to_decode  $\leftarrow$  positions_to_decode[:, :k]  $\triangleright$  Random positions to be predicted
10:  new_values  $\leftarrow$  pgm_predict(x, decoded_positions, pos_to_decode)
11:  x  $\leftarrow$  concat([x, new_values], dim=1)  $\triangleright$  Add new values to the sequence length dimension
12:  decoded_positions  $\leftarrow$  concat([decoded_positions, pos_to_decode], dim=1)
13:  positions_to_decode  $\leftarrow$  positions_to_decode[:, k:]  $\triangleright$  Remove the k decoded positions
14: end for
15: out  $\leftarrow$  reoder(x, decoded_positions)  $\triangleright$  Sort based on positions
16: return out
```

that we prevent information from flowing between different groups by masking entries in the attention matrix that correspond to pairs of tokens in different groups.

Decoder The decoder consists of cross-attention layers, where the keys and values are computed based on the output of the encoder. In contrast, the queries are computed using either the output of the GroupSwap layer (first block of the decoder) or the output of the previous decoder block. Importantly, there is no self-attention layer in the decoder, which allows efficient generation, as we can compute predictions solely for positions to decode.

4.1 The GroupSwap Layer

In the encoder, the information remains separated by group: tokens in group 0 only access information about tokens in group 0, and likewise for group 1. However, we want the neural network to make predictions for positions in group 1 based on information in group 0. Hence, we need to exchange information between groups, and we implement this exchange via a cross-attention layer that we call the GroupSap layer, visualized in Figure 3 (B). Let $\mathbf{g} \in \{0, 1\}^L$ be a binary vector that identifies the membership of the group at each position. After the GroupSwap layer, $\tilde{\mathbf{g}}$, the logical NOT of \mathbf{g} , tracks which group the information at each position originated from. The main design choice of the GroupSwap layer is how to initialize cross-attention queries. To avoid leakage, if $\tilde{\mathbf{g}}_i = 0$, then the query at position i should not depend on the tokens from partition 1.

Data-Independent Initialization Let $\mathbf{u} \in \mathbb{R}^H$ denote a learnable vector of dimension H . We initialize the queries by replicating \mathbf{u} along the sequence length and adding a fixed positional encoding, followed by a layer norm and a linear layer. Formally, let $V \in \mathbb{R}^{L \times H}$ denote the query initialization such that $V_{i,:}$ denotes the i -th row of V . Then,

$$V_{i,:} = W [\text{LN} (u + \text{pos}_{i,:}) + b], \quad (7)$$

where $W \in \mathbb{R}^{H \times H}$, $b \in \mathbb{R}^H$ are learnable parameters and LN denotes layer normalization [3]. The positional encoding is computed as

$$\text{pos}_{i,j} = \begin{cases} \cos\left(\frac{i}{10000^{2j/H}}\right) & \text{if } j < H/2 \\ \sin\left(\frac{i}{10000^{2j/H-1}}\right) & \text{otherwise} \end{cases} \quad (8)$$

Data-Dependent Initialization Let $X \in \mathbb{R}^{L \times H}$ denote the output of the encoder. We first compute a group-wise aggregation operation over the sequence length, such as logsumexp or mean, to obtain vectors $Y_0, Y_1 \in \mathbb{R}^H$, which represent the aggregation over groups 0 and 1, respectively. Then, the

| Model (LM1B) | Val. PPL ↓ | Model (OWT) | Val. PPL ↓ |
|-----------------------|--------------|-----------------------|--------------|
| <i>200k steps</i> | | <i>200k steps</i> | |
| MDLM | 34.29 | MDLM | 25.35 |
| MDLM (Compl. masking) | 30.87 | MDLM (Compl. masking) | 25.32 |
| PGM 8 / 4 | 32.83 | PGM 6 / 6 | 26.96 |
| PGM 10 / 2 | 33.55 | PGM 8 / 8 | <u>25.10</u> |
| PGM 4 / 8 | 32.84 | PGM 10 / 6 | 25.19 |
| PGM 6 / 6 | <u>32.69</u> | PGM 6 / 6 (dim. 1024) | 23.75 |
| PGM 6 / 6 (lsm) | 32.70 | | |
| PGM 6 / 6 (mean) | 33.89 | | |
| <i>1M steps</i> | | <i>1M steps</i> | |
| MDLM | 27.67 | MDLM | 23.07 |
| MDLM (Compl. masking) | 25.72 | MDLM (Compl. masking) | 22.98 |
| PGM 6 / 6 | <u>26.80</u> | PGM 8 / 8 | 22.70 |
| | | PGM 6 / 6 (dim. 1024) | 21.43 |

Table 1: Perplexity evaluations. Validation perplexity of the Masked Diffusion Language Model (MDLM) and PGMs (ours) on LM1B and OpenWebText (OWT). The row *MDLM (Compl. masking)* denotes an MDLM trained with the complementary masking strategy discussed in Section 5.3. The row *PGM k / m* denotes a PGM with k encoder and m decoder layers, and we highlighted the best PGM results in gray. *lsm* and *mean* denote the *logsumexp* and *mean* queries initializations (Section 4). **Takeaway:** using the same number of layers in the encoder and decoder, and data-independent queries performed best. On LM1B, our PGM reaches 1.95 lower perplexity than MDLM after 1M steps. On OWT, we grow the embedding dimension or the number of layers to outperform OWT.

data-dependent query initialization V' is computed as,

$$V'_{i,\cdot} = V_{i,\cdot} + \begin{cases} Y_1, & \text{if } g_i = 0 \\ Y_0 & \text{otherwise.} \end{cases} \quad (9)$$

5 Experiments

We investigated the performance of PGMs on language modeling and image generation tasks. We present complete details of the hyperparameters of the experiments in Appendix A.

5.1 Language Modeling on LM1B

Experimental setting. We closely follow the MDLM setup [36] and train models with a context length of 128 tokens. The shorter documents are padded to 128 tokens. We train a twelve-layer *Diffusion Transformer* [33] variant without time conditioning and compare it with our Partition Transformer (Section 4). We trained our models with a batch size of 512. We ablate on the architecture choices after training for 200k steps. The model with the best validation perplexity is further trained up to 1M steps and compared with MDLM.

Results Table 1 (left) shows that the use of as many layers in the encoder and decoder achieves the lowest validation perplexity. Additionally, data-independent queries slightly outperform data-dependent queries. After 1M steps, PGM reaches a validation perplexity of 1.95 lower than MDLM.

5.2 Language Modeling on OpenWebText

Experimental Settings We closely follow MDLM [36], and train models with a context length of 1024 tokens with sentence packing [35]. To ablate the architecture, we train models for 200k steps and compare them based on the validation perplexity. The two models with the best performance are further trained until 1M steps and compared with MDLM.

Architecture Ablations Table 1 (right) shows that, as for LM1B, allocating as many layers to the encoder and decoder achieves the best validation perplexity. However, we find that PGMs with the

same number of layers as MDLMs underperform in terms of validation perplexity. Therefore, we experiment with growing the model by using either more layers or growing the embedding dimension. Nonetheless, at inference, our larger PGMs achieve at least a 5x latency and throughput improvement against MDLM, as shown in Figure 1 and Table 5. Empirically, increasing the embedding dimension is more effective in terms of generation quality and speed. We hypothesize that the speedups in inference could make PGMs particularly relevant for the scaling of test-time computation [28, 53, 43, 51, 10, 5, 19], for example, in reasoning tasks.

5.3 Disentangling the Effect of the Architecture and Complementary Masking

To disentangle the contributions of PGM, we isolate the effect of complementary masking (subsection 3.2) by training a standard bidirectional transformer encoder with double batch size, using two complementary masked versions of each input sequence. This approach establishes an upper bound on potential performance gains, as it directly measures the impact of having complementary masks during gradient updates. We evaluated regular MDLM against MDLM with complementary masking in LM1B [9] and OpenWebText [18].

Table 1 shows that while complementary masking reduces the validation perplexity by 3.42 on LM1B, it offers negligible benefits on OWT. This difference might explain why PGMs with the same number of layers outperform MDLMs on LM1B, but not on OWT. In fact, on both data sets, there remains a gap between MDLM with complementary masking and PGM, which can be attributed to the neural network architecture being used. Since complementary masking does not lead to stronger models in OWT, we must increase the size of the model to match the validation perplexity of MDLM. However, recall that PGMs with more parameters generate higher-quality text and are significantly faster than MDLMs in inference (Figure 1). We investigate why complementary masking helps on LM1B but not on OWT in Appendix B.1.

5.4 Further Speedups via Distillation

PGM already delivers improvements over MDLM in both throughput and latency but we can push these gains further by applying “Self Distillation Through Time” (SDTT) [12]. For simplicity, we apply the distillation loss on partition 1, treating it as if it contained MASK tokens. This simple strategy allows us to use the original implementation of SDTT with few modifications. We leave the design of new distillation methods for PGMs to future work.

As shown in Figure 1, our best model, distilled with SDTT, can, in 16 steps, generate samples with better generative perplexity than MDLM would in 1024. *This induces a latency improvement of more than 280x over the original MDLM.* We compare PGM+SDTT with MDLM+SDTT in Appendix B. Additionally, PGM+SDTT achieves a 10.73x improvement over GPT-2 that uses KV-caching, while achieving a lower generative perplexity. See Table 5 and Table 6 for the exact numbers.

5.5 PGM on ImageNet

We evaluated PGM against MDLM on VQGAN tokenized images [15]. Our preliminary results show that while PGM still offers speedups on image data, the gains are less pronounced than for text generation. This difference stems primarily from the shorter sequence length in image generation. Our experiments are carried out on a smaller scale than a full MaskGIT implementation [8], with a comprehensive exploration of PGM architectures for images reserved for future work. Additional details are provided in Appendix B.

5.6 Downstream Performance

We compare the downstream performance of our models on the LAMBADA benchmark [32]. Table 2 shows that PGMs achieve a similar accuracy to MDLM, with a slight advantage to the PGM variant with more layers. Find more results on downstream tasks in Appendix B.4.

| Model | Acc. (%) ↑ |
|-----------------------|--------------|
| MDLM | 38.52 |
| PGM 8 / 8 | 46.98 |
| PGM 6 / 6 (dim. 1024) | 41.39 |

Table 2: **Accuracy on LAMBADA.**

6 Related Work

Diffusion on Discrete Space Although autoregressive models currently dominate text generation, recent advances in discrete diffusion [2, 27, 41, 36, 50, 40, 21] and discrete flow matching [7, 17] have demonstrated that MGMs can also generate text whose quality approaches samples from autoregressive models. Our work focuses primarily on the text domain, where our approach appears to be particularly promising. Although recent discrete diffusion and flow matching works focus on the modeling choices in defining the diffusion process, we focus on the neural network to improve inference efficiency. In principle, it should be straightforward to use PGMs with a score parameterization [29, 27, 55] instead of the mean parameterization [36, 41] that we use.

Accelerating Diffusion Models via Distillation Relatively few works on distillation have been explored for discrete diffusion models. “Self-Distillation Through Time” (SDTT) [12], inspired by “Progressive Distillation” [39] teaches the student MGM to match multiple sampling steps of the teacher MGM. “Di4C” [22] teaches the MGM denoiser x_θ the correlation between different positions. Leveraging the uncovered connection between discrete and continuous diffusion, “DUO” [37] proposes “discrete consistency distillation”, a distillation method for uniform discrete diffusion, inspired by consistency models [45]. “Di[M]O” [58] distills models with hybrid absorbing/uniform noise into one-step generators. In contrast, PGMs offer latency and throughput acceleration through a novel architecture, while remaining compatible with distillation, as discussed in Section 5.4.

Non-Autoregressive Language Models Any-order and any-subset autoregressive models [52, 31, 42, 20] learn an autoregressive distribution of tokens given arbitrary token subsets. In contrast, in this work, we accelerate MDLMs [36], which do not enforce causal attention on the tokens. “Block Diffusion” [1] (BD) proposes a hybrid architecture that interpolates between an autoregressive and a discrete diffusion model. Although BDs can generate tokens in parallel and allows KV caching [34], BDs still require generating tokens in a (block-) autoregressive fashion. In contrast, MDLM and PGMs can generate tokens in completely arbitrary orders.

Other Modalities In images, “MaskGIT” [8] demonstrates the power of MGMs. Trained on discrete tokens from a VQGAN [15], MaskGIT generates high-quality images in as few as 8 steps, leveraging the parallel token prediction abilities of the denoising neural network. This makes MaskGIT substantially faster than the autoregressive baseline [15]. MaskGIT has been successfully applied to other modalities, including videos [49, 54] and audio [11]. UniDisc [47] trains a multimodal MDLM that can process both text and discrete image tokens, while we focus on a single modality in this work.

7 Conclusion

We introduced Partition Generative Modeling (PGM), a novel approach to masked generative modeling that eliminates MASK tokens. PGM achieves significant improvements in inference speed while maintaining or improving generation quality. We show that PGMs are compatible with distillation methods devised for masked diffusion models, and present preliminary results on images. Future work could explore optimizations to the PGM architecture, investigating distillation techniques specifically designed for PGMs, and extending the approach to multimodal settings. Additionally, exploring how PGMs can be scaled to larger sizes and longer context lengths are interesting directions. Overall, PGM offers an interesting alternative to masked generative models, with particular advantages for applications where inference speed is critical.

8 Limitations

We need to increase the parameter count of our models to match the validation perplexity of the MDLM baseline when using a context length of 1024. Although PGMs are faster at inference, training is more costly (Appendix C). When applying SDTT to PGMs, we observe smaller improvements in Generative Perplexity than on MDLM. This suggests that the architecture can be further improved in future work. While Partition Generative Modeling is a general principle, the experiments on images are only preliminary, and whether the proposed transformer architecture can be applied in multimodal settings is a question to be studied in future work.

References

- [1] Marianne Arriola, Aaron Gokaslan, Justin T Chiu, Zhihan Yang, Zhixuan Qi, Jiaqi Han, Subham Sekhar Sahoo, and Volodymyr Kuleshov. Block diffusion: Interpolating between autoregressive and diffusion language models, 2025.
- [2] Jacob Austin, Daniel D. Johnson, Jonathan Ho, Daniel Tarlow, and Rianne van den Berg. Structured denoising diffusion models in discrete state-spaces, 2023.
- [3] Jimmy Lei Ba, Jamie Ryan Kiros, and Geoffrey E. Hinton. Layer normalization, 2016.
- [4] Victor Besnier, Mickael Chen, David Hurych, Eduardo Valle, and Matthieu Cord. Halton scheduler for masked generative image transformer, 2025.
- [5] Bradley Brown, Jordan Juravsky, Ryan Ehrlich, Ronald Clark, Quoc V. Le, Christopher Ré, and Azalia Mirhoseini. Large language monkeys: Scaling inference compute with repeated sampling, 2024.
- [6] Andrew Campbell, Joe Benton, Valentin De Bortoli, Tom Rainforth, George Deligiannidis, and Arnaud Doucet. A continuous time framework for discrete denoising models, 2022.
- [7] Andrew Campbell, Jason Yim, Regina Barzilay, Tom Rainforth, and Tommi Jaakkola. Generative flows on discrete state-spaces: Enabling multimodal flows with applications to protein co-design, 2024.
- [8] Huiwen Chang, Han Zhang, Lu Jiang, Ce Liu, and William T. Freeman. Maskgit: Masked generative image transformer, 2022.
- [9] Ciprian Chelba, Tomas Mikolov, Mike Schuster, Qi Ge, Thorsten Brants, Phillipp Koehn, and Tony Robinson. One billion word benchmark for measuring progress in statistical language modeling, 2014.
- [10] Lingjiao Chen, Jared Quincy Davis, Boris Hanin, Peter Bailis, Ion Stoica, Matei Zaharia, and James Zou. Are more llm calls all you need? towards scaling laws of compound inference systems, 2024.
- [11] Marco Comunità, Zhi Zhong, Akira Takahashi, Shiqi Yang, Mengjie Zhao, Koichi Saito, Yukara Ikemiya, Takashi Shibuya, Shusuke Takahashi, and Yuki Mitsufuji. Specmaskgit: Masked generative modeling of audio spectrograms for efficient audio synthesis and beyond, 2024.
- [12] Justin Deschenaux and Caglar Gulcehre. Beyond autoregression: Fast llms via self-distillation through time, 2025.
- [13] Jacob Devlin, Ming-Wei Chang, Kenton Lee, and Kristina Toutanova. Bert: Pre-training of deep bidirectional transformers for language understanding, 2019.
- [14] Sander Dieleman, Laurent Sartran, Arman Roshannai, Nikolay Savinov, Yaroslav Ganin, Pierre H. Richemond, Arnaud Doucet, Robin Strudel, Chris Dyer, Conor Durkan, Curtis Hawthorne, Rémi Leblond, Will Grathwohl, and Jonas Adler. Continuous diffusion for categorical data, 2022.
- [15] Patrick Esser, Robin Rombach, and Björn Ommer. Taming transformers for high-resolution image synthesis, 2021.
- [16] Leo Gao, Jonathan Tow, Baber Abbasi, Stella Biderman, Sid Black, Anthony DiPofi, Charles Foster, Laurence Golding, Jeffrey Hsu, Alain Le Noac’h, Haonan Li, Kyle McDonell, Niklas Muennighoff, Chris Ociepa, Jason Phang, Laria Reynolds, Hailey Schoelkopf, Aviya Skowron, Lintang Sutawika, Eric Tang, Anish Thite, Ben Wang, Kevin Wang, and Andy Zou. The language model evaluation harness, 07 2024.
- [17] Itai Gat, Tal Remez, Neta Shaul, Felix Kreuk, Ricky T. Q. Chen, Gabriel Synnaeve, Yossi Adi, and Yaron Lipman. Discrete flow matching, 2024.
- [18] Aaron Gokaslan and Vanya Cohen. Openwebtext corpus. <http://Skylion007.github.io/OpenWebTextCorpus>, 2019.

- [19] Sachin Goyal, Ziwei Ji, Ankit Singh Rawat, Aditya Krishna Menon, Sanjiv Kumar, and Vaishnavh Nagarajan. Think before you speak: Training language models with pause tokens, 2024.
- [20] Gabe Guo and Stefano Ermon. Reviving any-subset autoregressive models with principled parallel sampling and speculative decoding, 2025.
- [21] Etrit Haxholli, Yeti Z. Gurbuz, Oğul Can, and Eli Waxman. Efficient perplexity bound and ratio matching in discrete diffusion language models. In *The Thirteenth International Conference on Learning Representations*, 2025.
- [22] Satoshi Hayakawa, Yuhta Takida, Masaaki Imaizumi, Hiromi Wakaki, and Yuki Mitsufuji. Distillation of discrete diffusion through dimensional correlations, 2025.
- [23] Martin Heusel, Hubert Ramsauer, Thomas Unterthiner, Bernhard Nessler, and Sepp Hochreiter. Gans trained by a two time-scale update rule converge to a local nash equilibrium, 2018.
- [24] Vincent Tao Hu and Björn Ommer. [mask] is all you need, 2024.
- [25] Diederik P. Kingma and Jimmy Ba. Adam: A method for stochastic optimization, 2017.
- [26] Diederik P. Kingma, Tim Salimans, Ben Poole, and Jonathan Ho. Variational diffusion models, 2023.
- [27] Aaron Lou, Chenlin Meng, and Stefano Ermon. Discrete diffusion modeling by estimating the ratios of the data distribution, 2024.
- [28] Aman Madaan, Niket Tandon, Prakhar Gupta, Skyler Hallinan, Luyu Gao, Sarah Wiegrefe, Uri Alon, Nouha Dziri, Shrimai Prabhunoye, Yiming Yang, Shashank Gupta, Bodhisattwa Prasad Majumder, Katherine Hermann, Sean Welleck, Amir Yazdanbakhsh, and Peter Clark. Self-refine: Iterative refinement with self-feedback, 2023.
- [29] Chenlin Meng, Kristy Choi, Jiaming Song, and Stefano Ermon. Concrete score matching: Generalized score matching for discrete data, 2023.
- [30] Jingyang Ou, Shen Nie, Kaiwen Xue, Fengqi Zhu, Jiacheng Sun, Zhenguo Li, and Chongxuan Li. Your absorbing discrete diffusion secretly models the conditional distributions of clean data, 2025.
- [31] Arnaud Pannatier, Evann Courdier, and François Fleuret. Sigma-gpts: A new approach to autoregressive models, 2024.
- [32] Denis Paperno, Germán Kruszewski, Angeliki Lazaridou, Quan Ngoc Pham, Raffaella Bernardi, Sandro Pezzelle, Marco Baroni, Gemma Boleda, and Raquel Fernández. The lambada dataset: Word prediction requiring a broad discourse context, 2016.
- [33] William Peebles and Saining Xie. Scalable diffusion models with transformers, 2023.
- [34] Reiner Pope, Sholto Douglas, Aakanksha Chowdhery, Jacob Devlin, James Bradbury, Anselm Levskaya, Jonathan Heek, Kefan Xiao, Shivani Agrawal, and Jeff Dean. Efficiently scaling transformer inference, 2022.
- [35] Colin Raffel, Noam Shazeer, Adam Roberts, Katherine Lee, Sharan Narang, Michael Matena, Yanqi Zhou, Wei Li, and Peter J. Liu. Exploring the limits of transfer learning with a unified text-to-text transformer, 2023.
- [36] Subham Sekhar Sahoo, Marianne Arriola, Yair Schiff, Aaron Gokaslan, Edgar Marroquin, Justin T Chiu, Alexander Rush, and Volodymyr Kuleshov. Simple and effective masked diffusion language models, 2024.
- [37] Subham Sekhar Sahoo, Justin Deschenaux, Aaron Gokaslan, Guanghan Wang, Justin T Chiu, and Volodymyr Kuleshov. The diffusion duality. In *ICLR 2025 Workshop on Deep Generative Model in Machine Learning: Theory, Principle and Efficacy*, 2025.

- [38] Tim Salimans, Ian Goodfellow, Wojciech Zaremba, Vicki Cheung, Alec Radford, and Xi Chen. Improved techniques for training gans, 2016.
- [39] Tim Salimans and Jonathan Ho. Progressive distillation for fast sampling of diffusion models, 2022.
- [40] Yair Schiff, Subham Sekhar Sahoo, Hao Phung, Guanghan Wang, Sam Boshar, Hugo Dallatorre, Bernardo P. de Almeida, Alexander Rush, Thomas Pierrot, and Volodymyr Kuleshov. Simple guidance mechanisms for discrete diffusion models, 2025.
- [41] Jiaxin Shi, Kehang Han, Zhe Wang, Arnaud Doucet, and Michalis K. Titsias. Simplified and generalized masked diffusion for discrete data, 2025.
- [42] Andy Shih, Dorsa Sadigh, and Stefano Ermon. Training and inference on any-order autoregressive models the right way, 2022.
- [43] Charlie Snell, Jaehoon Lee, Kelvin Xu, and Aviral Kumar. Scaling llm test-time compute optimally can be more effective than scaling model parameters, 2024.
- [44] Jascha Sohl-Dickstein, Eric Weiss, Niru Maheswaranathan, and Surya Ganguli. Deep unsupervised learning using nonequilibrium thermodynamics. In Francis Bach and David Blei, editors, *Proceedings of the 32nd International Conference on Machine Learning*, volume 37 of *Proceedings of Machine Learning Research*, pages 2256–2265, Lille, France, 07–09 Jul 2015. PMLR.
- [45] Yang Song, Prafulla Dhariwal, Mark Chen, and Ilya Sutskever. Consistency models, 2023.
- [46] Jianlin Su, Yu Lu, Shengfeng Pan, Ahmed Murtadha, Bo Wen, and Yunfeng Liu. Roformer: Enhanced transformer with rotary position embedding, 2023.
- [47] Alexander Swerdlow, Mihir Prabhudesai, Siddharth Gandhi, Deepak Pathak, and Katerina Fragkiadaki. Unified multimodal discrete diffusion, 2025.
- [48] Ashish Vaswani, Noam Shazeer, Niki Parmar, Jakob Uszkoreit, Llion Jones, Aidan N. Gomez, Lukasz Kaiser, and Illia Polosukhin. Attention is all you need, 2023.
- [49] Ruben Villegas, Mohammad Babaeizadeh, Pieter-Jan Kindermans, Hernan Moraldo, Han Zhang, Mohammad Taghi Saffar, Santiago Castro, Julius Kunze, and Dumitru Erhan. Phenaki: Variable length video generation from open domain textual description, 2022.
- [50] Dimitri von Rütte, Janis Fluri, Yuhui Ding, Antonio Orvieto, Bernhard Schölkopf, and Thomas Hofmann. Generalized interpolating discrete diffusion, 2025.
- [51] Yangzhen Wu, Zhiqing Sun, Shanda Li, Sean Welleck, and Yiming Yang. An empirical analysis of compute-optimal inference for problem-solving with language models, 2024.
- [52] Zhilin Yang, Zihang Dai, Yiming Yang, Jaime Carbonell, Ruslan Salakhutdinov, and Quoc V. Le. Xlnet: Generalized autoregressive pretraining for language understanding, 2020.
- [53] Shunyu Yao, Dian Yu, Jeffrey Zhao, Izhak Shafran, Thomas L. Griffiths, Yuan Cao, and Karthik Narasimhan. Tree of thoughts: Deliberate problem solving with large language models, 2023.
- [54] Lijun Yu, Yong Cheng, Kihyuk Sohn, José Lezama, Han Zhang, Huiwen Chang, Alexander G. Hauptmann, Ming-Hsuan Yang, Yuan Hao, Irfan Essa, and Lu Jiang. Magvit: Masked generative video transformer, 2023.
- [55] Ruixiang Zhang, Shuangfei Zhai, Yizhe Zhang, James Thornton, Zijing Ou, Joshua Susskind, and Navdeep Jaitly. Target concrete score matching: A holistic framework for discrete diffusion, 2025.
- [56] Lingxiao Zhao, Xueying Ding, Lijun Yu, and Leman Akoglu. Unified discrete diffusion for categorical data, 2024.

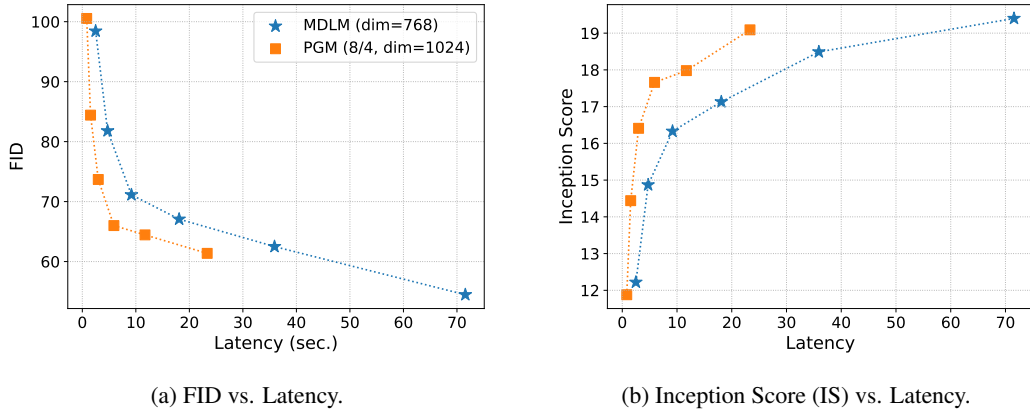


Figure 4: Comparison of the performance of PGMs and MDLMs when modeling discrete image tokens. When the inference budget is limited, PGMs outperform MDLMs. Note that we do *not* target state-of-the-art result in this experiment, rather we compare the regular MDLM and PGM that were used in experiments on text.

- [57] Kaiwen Zheng, Yongxin Chen, Hanzi Mao, Ming-Yu Liu, Jun Zhu, and Qinsheng Zhang. Masked diffusion models are secretly time-agnostic masked models and exploit inaccurate categorical sampling, 2025.
- [58] Yuanzhi Zhu, Xi Wang, Stéphane Lathuilière, and Vicky Kalogeiton. Di[M]o: Distilling masked diffusion models into one-step generator, 2025.

A Experimental Details

We trained all models from scratch rather than using the pre-trained models released by the MDLM authors. Our models achieve comparable performance to the original work. On LM1B, we obtain a validation perplexity of 27.67 after 1M steps (compared to MDLM’s reported 27.04), while on OWT, we reach 23.07 (versus MDLM’s 23.21).

Minor differences can be expected since estimating the perplexity of diffusion language models involves a Monte-Carlo approximation of the NELBO (Equation 4) with finitely many samples. Although we used libraries (e.g PyTorch) with the same version as MDLM, differences in compute environments and underlying software stacks may also contribute to these variations. Since the performance gap is small, we are confident that we used the code of MDLM correctly.

A.1 LM1B

For the LM1B dataset, we employed the bert-base-uncased tokenizer with a context length of 128 tokens, padding shorter sequences to 128 tokens. Our architecture consisted of a Diffusion Transformer (DiT) with 12 transformer blocks, 12 attention heads, a hidden dimension of 768 and a dropout rate of 0.1. We optimized the model using Adam [25] (learning rate $3e-4$, betas of (0.9, 0.999), epsilon $1e-8$) without weight decay. We based our implementation on the official MDLM codebase. We trained with a global batch size of 512 across 8 GPUs (2 nodes with 4 GPUs), gradient clipping at 1.0, and a constant learning rate with 2,500 steps of linear warmup. We trained for 1 million steps with an EMA rate of 0.9999. Besides the neural network hyperparameters, the other parameters were unchanged when training the PGM.

A.2 OWT

For the OpenWebText (OWT) dataset, we used the GPT-2 tokenizer with a context length of 1024 tokens. Our architecture consisted of a Diffusion Transformer (DiT) with 12 transformer blocks, 12 attention heads, a hidden dimension of 768, and a dropout rate of 0.1. We optimized the model using Adam [25] with a learning rate of $3e-4$, betas of (0.9, 0.999), and epsilon of $1e-8$, without weight

Table 3: Latency and throughput for a single training step of the MDLMs and PGMs, computed on a single A100-SXM4-80GB GPU. On LM1B, PGM introduce a negligible overhead over MDLM. On OWT, our PGM with 6 encoder and decoder layer and an embedding dimension of 1024 achieves around 75% of the training throughput of MDLM. Recall that at inference, the same PGM is around 5x faster than MDLM. On ImageNet, the PGM achieves 68% of the training throughput of MDLM.

| Model | Forward Pass | | Forward + Backward | |
|---|--------------|-------------------|--------------------|----------------|
| | Latency (ms) | Seq/sec | Latency (ms) | Seq/Sec |
| <i>LM1B (context length 128, batch size 64, trained on 8 GPUs)</i> | | | | |
| MDLM | 0.03 ± 0.00 | 1'978.87 ± 44.21 | 0.08 ± 0.00 | 714.80 ± 15.47 |
| PGM 6 / 6 | 0.03 ± 0.00 | 1'966.60 ± 102.14 | 0.08 ± 0.00 | 794.42 ± 18.81 |
| <i>OpenWebText (context length 1024, batch size 32, trained on 16 GPUs)</i> | | | | |
| MDLM | 0.13 ± 0.00 | 233.28 ± 2.58 | 0.39 ± 0.00 | 80.86 ± 0.15 |
| PGM 8 / 8 | 0.17 ± 0.00 | 188.07 ± 0.75 | 0.47 ± 0.00 | 68.04 ± 0.08 |
| PGM 6 / 6 (dim. 1024) | 0.18 ± 0.00 | 176.47 ± 0.65 | 0.50 ± 0.00 | 62.85 ± 0.19 |
| <i>ImageNet (context length 257, batch size 128, trained on 4 GPUs)</i> | | | | |
| MDLM | 0.11 ± 0.01 | 1'066.98 ± 11.13 | 0.33 ± 0.00 | 385.77 ± 0.67 |
| PGM 8 / 4 (dim=1024) | 0.17 ± 0.01 | 727.43 ± 40.58 | 0.45 ± 0.02 | 279.15 ± 8.74 |

decay. We trained with a global batch size of 512 across 16 GPUs (4 nodes with 4 GPUs). We applied gradient clipping at 1.0 and used a constant learning rate schedule with 2,500 steps of linear warmup. The model was trained for 1 million steps with an EMA rate of 0.9999. Besides the neural network hyperparameters, the other parameters were unchanged when training the PGM.

A.3 ImageNet

For the ImageNet dataset, we used a pre-trained VQGAN tokenizer [15, 4] with a downsampling factor of 16, resulting in 256 tokens per image (16x16 grid). Our architecture consisted of a Diffusion Transformer (DiT) with 12 transformer blocks, 12 attention heads, a hidden dimension of 768, and a dropout rate of 0.1. We optimized the model using Adam with a learning rate of 3e-4, betas of (0.9, 0.999), and epsilon of 1e-8, without weight decay. We trained with a global batch size of 512 across 4 GPUs on a single node. We applied gradient clipping at 1.0 and used a constant learning rate schedule with 2,500 steps of linear warmup. The model was trained for 1 million steps with an EMA rate of 0.9999. Instead of the whole ImageNet, we used the Imagenet256 dataset, downloaded from Kaggle, as used in prior work [24]. Besides the neural network hyperparameters, the other parameters were unchanged when training the PGM. Since this version of the dataset does not have a predefined validation set, we use 50'000 randomly selected ones as validation. We train our models to be class unconditional. We use a vocabulary with 16'386 values, representing the 16'384 values from the VQGAN codebook [15, 4], a MASK token and a special "BOS" token.

A.4 Impact of Numerical Precision on Sampling

Prior work [57] identified that Masked Diffusion Models often achieve lower generative perplexity results because of underflow in the logits when sampling using 16-bit precision. The resulting decrease in token diversity can make evaluations based solely on generative perplexity misleading. To ensure fair comparison across all models, we cast all logits to FP64 before sampling for every model in our experiments, including GPT-2.

A.5 Sample-Based Evaluation

Generative Perplexity We evaluate the quality of the generated text using the generative perplexity as our primary metric, following previous work [27, 36, 12]. The generative perplexity measures how well a reference model (in our case, GPT-2 Large) can predict the next token in sequences generated by our models. Specifically, we generate 1'024 samples from each model being evaluated. For each

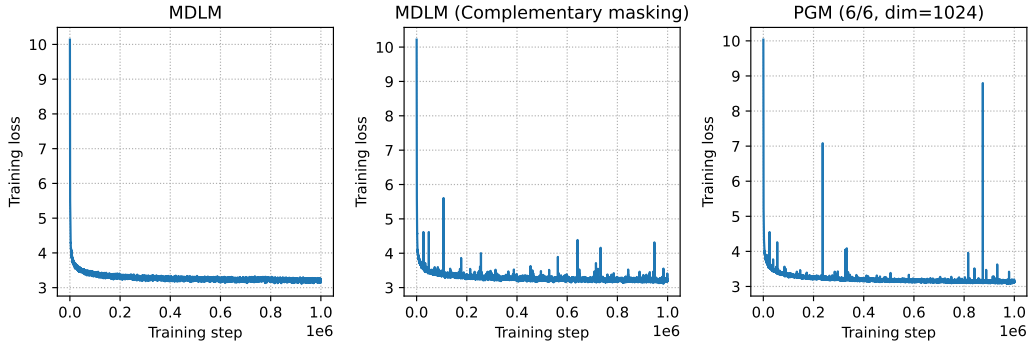


Figure 5: Training loss of MDLM, MDLM with Complementary Masking (Section 5.3) and PGM. Complementary masking seems to introduce spikes in the loss, even though it did not cause the models to diverge.

generated sample, we compute the generative perplexity using GPT-2 Large as follows:

$$\text{Perplexity} = \exp \left(-\frac{1}{N} \sum_{i=1}^N \log p_{\text{GPT-2 Large}}(x_i | x_{<i}) \right), \quad (10)$$

where L is the length of the sequence, x_i is the i -th token, and $p_{\text{GPT-2 Large}}(x_i | x_{<i})$ is the probability assigned by GPT-2 Large to token x_i given the preceding tokens $x_{<i}$.

Unigram Entropy Unfortunately, a low generative perplexity can be achieved by generating repetitive text. To catch such cases, we compute the average unigram entropy of the generated samples:

$$\text{Unigram Entropy} = -\frac{1}{N} \sum_{i=1}^N \sum_{v \in \mathcal{X}} \frac{c(v, \mathbf{x}^{(i)})}{L} \log \frac{c(v, \mathbf{x}^{(i)})}{L}, \quad (11)$$

where \mathcal{X} is the vocabulary, v is a token of the vocabulary, and $c(v, \mathbf{x})$ is the empirical appearance count of the token v in the sequence \mathbf{x} . Low unigram entropy helps us to catch degenerate generation, as shown in prior work [14].

Fréchet Inception Distance and Inception Score On image generation tasks, we evaluate the quality of samples using the Fréchet Inception Distance (FID) [23] and Inception Score (IS) [38]. For efficiency, we use 10'000 generated images to compute those metrics, instead of the more common 50'000.

B Additional Results

B.1 Impact of Context Length on the Effectiveness of Complementary Masking

There are three key differences between our experiments on LM1B and OWT. First, we used different tokenizers: `bert-base-uncased` for LM1B and GPT2's tokenizer for OWT, following the setup of MDLM [36]. Second, the context lengths differ significantly: 128 tokens for LM1B versus 1024 for OWT. Third, we train on different datasets, which might have different characteristics.

We observed that complementary masking helps when training on OWT using a shorter context length of 128 tokens with the GPT-2 tokenizer. Indeed, after the 200k training step, the MDLM with complementary masking achieved a validation PPL of 37.92, outperforming the standard MDLM, which reached 39.90. This evidence suggests PGMs can be particularly beneficial for applications with short context lengths.

B.2 MDLM+SDTT vs PGM+SDTT

The precision of logits during sampling can have a significant effect on sample quality, as noted in Appendix A.4. Hence, we cast all logits to FP64 prior to sampling, unlike the original MDLM and SDTT implementations.

Using a higher precision also impacts the distillation process, which works by compressing two sampling steps into one. Therefore, generating the teacher targets using higher precision increases the final generative perplexity compared to the results reported by SDTT, as shown in Table 7 and Figure 6. However, since we made only this minimal change while otherwise using the official SDTT implementation, we are confident in the validity of our results.

For a fair comparison, we re-distilled our MDLM checkpoints with SDTT using higher precision. Specifically, we used FP32 precision when generating teacher targets, allowing us to compare MDLM+SDTT against our PGM+SDTT with the lowest generative perplexity. We observe that after distillation, the entropy of samples generated with MDLM+SDTT decreases much more than the entropy of samples generated by PGM+SDTT. Figure 6 shows that MDLM+SDTT achieves lower generative perplexity than PGM+SDTT, which indicates opportunities for further architectural improvements in future work.

B.3 Training Stability

Complementary masking introduces occasional spikes in the training loss in both MDLMs and PGMs, as shown in Figure 5. This phenomenon should be kept in mind when scaling PGMs to larger sizes. Despite these spikes, all runs converged on the first attempt. We observed different precision requirements between models. MDLMs performed slightly better with BF16 precision, while PGMs showed improved results when using FP32 precision for the PyTorch Lightning trainer. Note that in both cases, the neural network backbone computations were consistently performed using mixed precision (BF16). Hence, the precision difference only affected operations outside the model, such as loss calculations.

B.4 Additional Downstream Tasks

Table 4 shows more downstream evaluation results, where PGM outperforms MDLM on all but one benchmark, where the difference is small. We compare the models using the `lm-eval-harness` library [16]. The `lm-eval-harness` library was designed for autoregressive language models and needs to be adapted for MDLM. For multiple choice questions, `lm-eval-harness` relies on a function that computes the log-likelihood of each answer y_i given a prefix \mathbf{x} . The model computes $p(y_i|\mathbf{x})$ for each possible answer i and choosing the one with the highest log-likelihood.

Adapting `lm-eval-harness` for MDLM While `lm-eval-harness` uses the log-likelihood of the continuation, the NELBO objective (Equation 4) bounds the log-likelihood of the *complete* sequence $(\mathbf{x}, \mathbf{y}_i)$. However, we only need to know which continuation achieves the highest log-likelihood, not to compute the exact log-likelihood. Therefore, using Bayes’ theorem, we note that

$$\log p(\mathbf{y}_i|\mathbf{x}) = \log p(\mathbf{x}, \mathbf{y}_i) - \log p(\mathbf{x}) \propto \log p(\mathbf{x}, \mathbf{y}_i), \tag{12}$$

since $\log p(\mathbf{x})$ is constant with respect to \mathbf{y}_i .

C Computational Costs

This section presents the computational costs associated with the models reported in this paper. We exclude costs associated with exploratory experiments that yielded inferior results and were not included in this manuscript.

C.1 Training Costs

Training PGMs is currently slower than training MGMs since we use `torch.sdpa` with dense tensor masks. Future work should explore efficient kernels to address this limitation. Despite this training

| Model | LAMBADA | ARC-e | ARC-c | HSwag | MathQA | PIQA | WinoG |
|------------------|--------------|--------------|--------------|--------------|--------------|--------------|--------------|
| MDLM | 38.52 | 34.26 | 24.66 | 31.54 | 20.70 | 57.89 | 51.93 |
| PGM 8 / 8 | 46.98 | 37.37 | 24.06 | 33.10 | 21.24 | 59.09 | 51.30 |
| PGM 6 / 6 (1024) | 41.39 | 38.80 | 22.95 | 33.92 | 21.71 | 61.43 | 54.30 |

Table 4: Accuracy on downstream tasks. We evaluate MDLM and PGM on LAMBADA, ARC Easy and Challenge, HellaSwag, MathQA, PIQA, and WinoGrande. Both models show comparable performance across tasks. PGM outperform MDLM on all but one benchmark, where the difference between MDLM and PGM 8 / 8 is small.

overhead, recall that we focus on the inference efficiency. We measure the latency and throughput using a single NVIDIA A100-SXM4-80GB GPU, with results reported in Table 3. We compute the mean and standard deviation over 100 batches after 2 warmup batches.

The total training duration approximately equals the per-step latency multiplied by the number of steps. Experiments with complementary masking required twice the computational resources due to larger batch sizes and gradient accumulation. Training times for 1M steps varied by dataset: approximately 22 hours for LM1B, 4.5 days for OWT, and 3.8 days for ImageNet.

C.2 Inference Costs

We evaluate the inference efficiency of PGMs compared to MDLMs and GPT-2 with KV caching. As shown in Figure 1, PGMs achieve around 5- 5.5x improvements in latency and throughput over MDLM while reaching superior generative perplexity. For inference measurements, we use a single NVIDIA A100-SXM4-80GB GPU and report both latency and throughput metrics. The efficiency gain stems from the ability of PGMs to process only unmasked tokens during inference, as illustrated in Figure 2. Table 5 compares MDLM and PGMs on the generative perplexity, unigram entropy, latency, and throughput. We compute mean and standard deviation of the latency and throughput over 20 batches after two warmup batches.

C.3 Licensing

Our code and model artifacts will be released under the MIT license. The OWT dataset [18] is available under the Apache License 2.0. We were unable to identify a specific license for the LM1B dataset [9]. The images in ImageNet remain the property of their respective copyright holders.

Algorithm 2 MDLM-equivalent sampling for PGMs.

```
1: Input: Batch size BS, number of steps K, model length L, special BOS index
2: Output: Generated samples x
3: x  $\leftarrow$  empty_tensor(BS, 1)  $\triangleright$  Initialize
4: x[:, 0]  $\leftarrow$  BOS  $\triangleright$  Set BOS as first token
5: k  $\leftarrow$  L/K  $\triangleright$  Number of tokens to denoise at each step
6: clean_positions  $\leftarrow$  zeros(BS, 1)  $\triangleright$  Keep track of clean and noisy positions
7: concrete_lengths  $\leftarrow$  ones(BS, 1)  $\triangleright$  Keep track of the actual length of each sequence (some are padded).
8: noisy_positions  $\leftarrow$  1 + rand_row_perm(BS, L-1)
9: for _ in range(K) do
10:     n_denoise_per_seq, noisy_pos_input  $\leftarrow$  sample_noisy(noisy_positions, k)  $\triangleright$  Algorithm 3
11:     new_values  $\leftarrow$  pgm_predict(x, clean_positions, noisy_pos_input)
12:     x, clean_positions, noisy_positions, concrete_lengths  $\leftarrow$  extract_predictions(
13:         x,  $\triangleright$  Algorithm 4
14:         clean_positions,
15:         noisy_positions,
16:         noisy_pos_input,
17:         concrete_lengths,
18:         n_denoise_per_seq,
19:         new_values)
20: end for
21: out  $\leftarrow$  reoder(x, clean_positions)  $\triangleright$  Sort based on clean_positions
22: return out
```

Algorithm 3 Sample the number of tokens to denoise from a binomial distribution and pad the input.

```
1: Input: Noisy positions tensor, probability of denoising prob_denoise, model length L, concrete lengths tensor
2: Output: Noisy positions to denoise
3: n_denoise_per_seq  $\leftarrow$  binomial(BS, L, prob_denoise)  $\triangleright$  Sample from binomial distribution
4: n_denoise_per_seq  $\leftarrow$  min(n_denoise_per_seq, L - concrete_lengths)  $\triangleright$  Don't denoise more than available
5: denoise_seq_len  $\leftarrow$  max(n_denoise_per_seq, 0)  $\triangleright$  Maximum number of tokens to denoise
6: if denoise_seq_len = 0 then
7:     return empty_tensor()  $\triangleright$  Nothing to denoise
8: end if
9: noisy_pos_input  $\leftarrow$  noisy_positions[:, :denoise_seq_len]  $\triangleright$  Some predictions won't be used
10: return n_denoise_per_seq, noisy_pos_input
```

NeurIPS Paper Checklist

1. Claims

Question: Do the main claims made in the abstract and introduction accurately reflect the paper's contributions and scope?

Answer: [\[Yes\]](#)

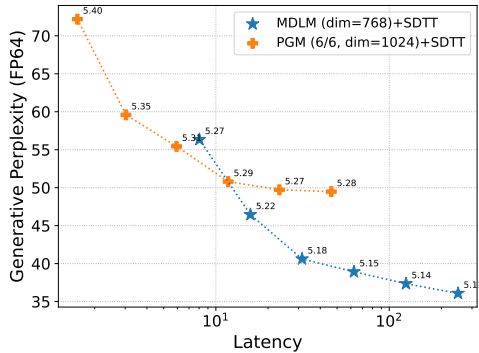
Justification: Yes, we propose an alternative to Masked Generative Modeling that does not require processing MASK tokens at training and inference. We show inference efficiency gains on two text datasets commonly used in prior work on discrete diffusion. We also demonstrate favorable speed-ups against MDLM when modeling discrete image tokens. On text, we report the validation perplexity, generative perplexity, throughput and latency to support our claims. On image, we report the FID, IS, throughput and latency.

Guidelines:

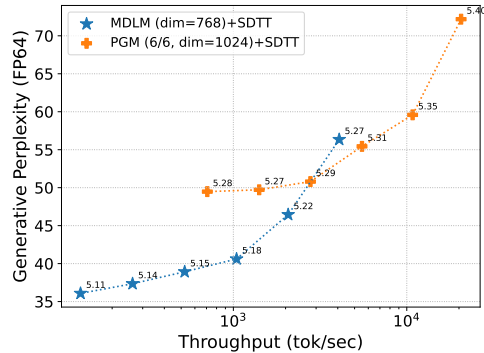
- The answer NA means that the abstract and introduction do not include the claims made in the paper.

Algorithm 4 Extract the correct number of predictions per sequence

```
1: Input: x, concrete_lengths, n_denoise_per_seq, denoised_token_values, clean_positions,
   noisy_positions, noisy_pos_input
2: Output: Updated x, clean_positions, noisy_positions, concrete_lengths
3: new_concrete_lengths  $\leftarrow$  concrete_lengths + n_denoise_per_seq  $\triangleright$  Update sequence lengths
4: n_tok_to_add  $\leftarrow$  max(new_concrete_lengths) - shape(x, 1)  $\triangleright$  Calculate padding needed
5: if n_tok_to_add > 0 then
6:   pad  $\leftarrow$  zeros(BS, n_tok_to_add)  $\triangleright$  Create padding tensor
7:   x  $\leftarrow$  concat(x, pad, dim=1)  $\triangleright$  Pad the sequences
8:   clean_positions  $\leftarrow$  concat(clean_positions, pad, dim=1)  $\triangleright$  Pad the positions
9: end if
10: for i in range(BS) do
11:   if n_denoise_per_seq[i] = 0 then
12:     continue  $\triangleright$  Skip if no tokens to denoise
13:   end if
14:   x[i, concrete_lengths[i]:new_concrete_lengths[i]]  $\leftarrow$ 
15:     denoised_token_values[i, :n_denoise_per_seq[i]]
16:   clean_positions[i, concrete_lengths[i]:new_concrete_lengths[i]]  $\leftarrow$ 
17:     noisy_pos_input[i, :n_denoise_per_seq[i]]
18:   noisy_positions[i, :shape(noisy_positions, 1) - n_denoise_per_seq[i]]  $\leftarrow$ 
19:     noisy_positions[i, n_denoise_per_seq[i]:]
20: end for
21: return x, clean_positions, noisy_positions, new_concrete_lengths
```



(a) Generative PPL vs. Latency.



(b) Throughput vs. Latency.

Figure 6: Comparison of PGMs and MDLMs *after distillation with SDTT* on OWT. We see that PGM+SDTT achieve higher generative perplexity than MDLM+SDTT. This is not entirely surprising since SDTT was devised for MDLM. Designing better distillation methods for PGMs is left for future work.

- The abstract and/or introduction should clearly state the claims made, including the contributions made in the paper and important assumptions and limitations. A No or NA answer to this question will not be perceived well by the reviewers.
- The claims made should match theoretical and experimental results, and reflect how much the results can be expected to generalize to other settings.
- It is fine to include aspirational goals as motivation as long as it is clear that these goals are not attained by the paper.

2. Limitations

Question: Does the paper discuss the limitations of the work performed by the authors?

Answer: [Yes]

Justification: We discuss the limitations in Section 8.

Table 5: Sample quality and efficiency on OpenWebText with different numbers of sampling steps. We generate sequences of 1024 tokens with a batch size of 32 to measure the latency and throughput. PGM 6 / 6 with a hidden dimension of 1024 and uniform sampling achieves at least a 5x latency and throughput improvement over MDLM, with better generative perplexity and matching entropy.

| Model | Gen. PPL ↓ | Entropy ↑ | Latency ↓ (ms) | Throughput ↑ (tok/s) |
|--|------------|-----------|-------------------|-------------------------|
| <i>MDLM</i> | | | | |
| 32 steps | 192.31 | 5.73 | 8.037 ± 0.01 | 4'077.08 ± 3.06 |
| 64 steps | 142.58 | 5.69 | 15.82 ± 0.01 | 2'070.67 ± 0.69 |
| 128 steps | 122.89 | 5.67 | 31.41 ± 0.01 | 1'043.22 ± 0.16 |
| 256 steps | 113.96 | 5.66 | 62.54 ± 0.01 | 523.90 ± 0.06 |
| 512 steps | 109.05 | 5.64 | 124.94 ± 0.16 | 262.26 ± 0.33 |
| 1024 steps | 106.75 | 5.64 | 249.31 ± 0.11 | 131.42 ± 0.05 |
| <i>PGM 8 / 8 (uniform sampling)</i> | | | | |
| 32 steps | 189.02 | 5.73 | 1.55 ± 0.01 | 21'120.99 ± 83.59 |
| 64 steps | 143.79 | 5.69 | 3.00 ± 0.01 | 10'914.91 ± 41.69 |
| 128 steps | 122.21 | 5.66 | 5.86 ± 0.02 | 5'585.57 ± 24.49 |
| 256 steps | 112.48 | 5.65 | 11.64 ± 0.03 | 2'814.99 ± 9.33 |
| 512 steps | 108.76 | 5.64 | 22.98 ± 0.02 | 1'425.89 ± 1.61 |
| 1024 steps | 107.03 | 5.63 | 45.84 ± 0.03 | 714.71 ± 0.50 |
| <i>PGM 8 / 8 (non uniform sampling)</i> | | | | |
| 32 steps | 194.09 | 5.73 | 2.07 ± 0.02 | 15'764.09 ± 192.12 |
| 64 steps | 143.60 | 5.69 | 3.90 ± 0.07 | 8'405.14 ± 158.01 |
| 128 steps | 124.38 | 5.67 | 7.41 ± 0.08 | 4'419.77 ± 53.27 |
| 256 steps | 116.85 | 5.66 | 14.73 ± 0.19 | 2'223.6372 ± 28.47 |
| 512 steps | 111.11 | 5.64 | 28.15 ± 0.32 | 1'163.79 ± 13.25 |
| 1024 steps | 108.24 | 5.63 | 54.62 ± 0.66 | 599.97 ± 7.27 |
| <i>PGM 6 / 6 (dim. 1024, uniform sampling)</i> | | | | |
| 32 steps | 185.16 | 5.73 | 1.59 ± 0.01 | 20'569.99 ± 95.63 |
| 64 steps | 138.87 | 5.70 | 3.03 ± 0.01 | 10'805.31 ± 14.11 |
| 128 steps | 116.95 | 5.67 | 5.93 ± 0.01 | 5'518.09 ± 13.46 |
| 256 steps | 108.51 | 5.65 | 11.77 ± 0.01 | 2'782.78 ± 3.46 |
| 512 steps | 101.94 | 5.63 | 23.25 ± 0.01 | 1'408.88 ± 1.05 |
| 1024 steps | 99.64 | 5.62 | 46.31 ± 0.02 | 707.52 ± 0.34 |
| <i>PGM 6 / 6 (dim. 1024, non-uniform sampling)</i> | | | | |
| 32 steps | 191.30 | 5.74 | 2.12 ± 0.07 | 15'415.56 ± 467.20 |
| 64 steps | 138.67 | 5.69 | 3.940 ± 0.06 | 8'318.72 ± 135.47 |
| 128 steps | 118.17 | 5.67 | 7.60 ± 0.09 | 4'311.80 ± 54.92 |
| 256 steps | 108.93 | 5.65 | 14.84 ± 0.20 | 2'207.71 ± 29.71 |
| 512 steps | 105.41 | 5.64 | 28.56 ± 0.33 | 1'147.17 ± 13.47 |
| 1024 steps | 102.93 | 5.62 | 55.50 ± 0.36 | 590.37 ± 3.85 |

Guidelines:

- The answer NA means that the paper has no limitation while the answer No means that the paper has limitations, but those are not discussed in the paper.
- The authors are encouraged to create a separate "Limitations" section in their paper.
- The paper should point out any strong assumptions and how robust the results are to violations of these assumptions (e.g., independence assumptions, noiseless settings, model well-specification, asymptotic approximations only holding locally). The authors should reflect on how these assumptions might be violated in practice and what the implications would be.
- The authors should reflect on the scope of the claims made, e.g., if the approach was only tested on a few datasets or with a few runs. In general, empirical results often depend on implicit assumptions, which should be articulated.

- The authors should reflect on the factors that influence the performance of the approach. For example, a facial recognition algorithm may perform poorly when image resolution is low or images are taken in low lighting. Or a speech-to-text system might not be used reliably to provide closed captions for online lectures because it fails to handle technical jargon.
- The authors should discuss the computational efficiency of the proposed algorithms and how they scale with dataset size.
- If applicable, the authors should discuss possible limitations of their approach to address problems of privacy and fairness.
- While the authors might fear that complete honesty about limitations might be used by reviewers as grounds for rejection, a worse outcome might be that reviewers discover limitations that aren't acknowledged in the paper. The authors should use their best judgment and recognize that individual actions in favor of transparency play an important role in developing norms that preserve the integrity of the community. Reviewers will be specifically instructed to not penalize honesty concerning limitations.

3. Theory assumptions and proofs

Question: For each theoretical result, does the paper provide the full set of assumptions and a complete (and correct) proof?

Answer: [NA]

Justification: We not present theoretical results.

Guidelines:

- The answer NA means that the paper does not include theoretical results.
- All theorems, formulas, and proofs in the paper should be numbered and cross-referenced.
- All assumptions should be clearly stated or referenced in the statement of any theorems.
- The proofs can either appear in the main paper or the supplemental material, but if they appear in the supplemental material, the authors are encouraged to provide a short proof sketch to provide intuition.
- Inversely, any informal proof provided in the core of the paper should be complemented by formal proofs provided in the appendix or supplemental material.
- Theorems and Lemmas that the proof relies upon should be properly referenced.

4. Experimental result reproducibility

Question: Does the paper fully disclose all the information needed to reproduce the main experimental results of the paper to the extent that it affects the main claims and/or conclusions of the paper (regardless of whether the code and data are provided or not)?

Answer: [Yes]

Justification: We built our project on top of MDLM [36], which has an open-source code available on GitHub. We use the same data preparation steps, on well-established datasets (LM1B, OpenWebText and ImageNet), that are widely available for download. Additionally, we report the hyperparameters in Appendix A. We only ablate on the hyperparameters of the proposed architecture, and use the same optimizer, learning rate scheduler and dropout rate as MDLM to save costs. We also provide Python-like sampling pseudocode in Algorithm 1 and Algorithm 2. We also provide the mathematical expressions that our new neural network layers implement. Finally, upon de-anonymization, we will release our code and checkpoints.

Guidelines:

- The answer NA means that the paper does not include experiments.
- If the paper includes experiments, a No answer to this question will not be perceived well by the reviewers: Making the paper reproducible is important, regardless of whether the code and data are provided or not.
- If the contribution is a dataset and/or model, the authors should describe the steps taken to make their results reproducible or verifiable.

- Depending on the contribution, reproducibility can be accomplished in various ways. For example, if the contribution is a novel algorithm, describing the algorithm fully might suffice, or if the contribution is a specific model and empirical evaluation, it may be necessary to either make it possible for others to replicate the model with the same dataset, or provide access to the model. In general, releasing code and data is often one good way to accomplish this, but reproducibility can also be provided via detailed instructions for how to replicate the results, access to a hosted model (e.g., in the case of a large language model), releasing of a model checkpoint, or other means that are appropriate to the research performed.
- While NeurIPS does not require releasing code, the conference does require all submissions to provide some reasonable avenue for reproducibility, which may depend on the nature of the contribution. For example
 - (a) If the contribution is primarily a new algorithm, the paper should make it clear how to reproduce that algorithm.
 - (b) If the contribution is primarily a new model architecture, the paper should describe the architecture clearly and fully.
 - (c) If the contribution is a new model (e.g., a large language model), then there should either be a way to access this model for reproducing the results or a way to reproduce the model (e.g., with an open-source dataset or instructions for how to construct the dataset).
 - (d) We recognize that reproducibility may be tricky in some cases, in which case authors are welcome to describe the particular way they provide for reproducibility. In the case of closed-source models, it may be that access to the model is limited in some way (e.g., to registered users), but it should be possible for other researchers to have some path to reproducing or verifying the results.

5. Open access to data and code

Question: Does the paper provide open access to the data and code, with sufficient instructions to faithfully reproduce the main experimental results, as described in supplemental material?

Answer: [Yes]

Justification: The data preparation steps are the same as used in MDLM, hence are available in open access. The code to reproduce our results is attach as a zip file, along with bash scripts to explain how to use the code. Some small variations of the scripts are not included, for example when the only change is to vary the number of layers in the encoder and decoder for the PGM. Indeed, we provide bash scripts that clearly shows where to set the number of layers, hence training with a different number of layer is a matter of changing two lines of the run command.

Guidelines:

- The answer NA means that paper does not include experiments requiring code.
- Please see the NeurIPS code and data submission guidelines (<https://nips.cc/public/guides/CodeSubmissionPolicy>) for more details.
- While we encourage the release of code and data, we understand that this might not be possible, so "No" is an acceptable answer. Papers cannot be rejected simply for not including code, unless this is central to the contribution (e.g., for a new open-source benchmark).
- The instructions should contain the exact command and environment needed to run to reproduce the results. See the NeurIPS code and data submission guidelines (<https://nips.cc/public/guides/CodeSubmissionPolicy>) for more details.
- The authors should provide instructions on data access and preparation, including how to access the raw data, preprocessed data, intermediate data, and generated data, etc.
- The authors should provide scripts to reproduce all experimental results for the new proposed method and baselines. If only a subset of experiments are reproducible, they should state which ones are omitted from the script and why.
- At submission time, to preserve anonymity, the authors should release anonymized versions (if applicable).

- Providing as much information as possible in supplemental material (appended to the paper) is recommended, but including URLs to data and code is permitted.

6. Experimental setting/details

Question: Does the paper specify all the training and test details (e.g., data splits, hyperparameters, how they were chosen, type of optimizer, etc.) necessary to understand the results?

Answer: [Yes]

Justification: We build our project on top of MDLM [36], which has an open-source code available on GitHub. We use the same data preparation steps, on well-established datasets (LM1B, OpenWebText, ImageNet), that are widely available on internet. Additionally, we report the most important hyperparameters in the experiment section, and all hyperparameters in Appendix A.

Guidelines:

- The answer NA means that the paper does not include experiments.
- The experimental setting should be presented in the core of the paper to a level of detail that is necessary to appreciate the results and make sense of them.
- The full details can be provided either with the code, in appendix, or as supplemental material.

7. Experiment statistical significance

Question: Does the paper report error bars suitably and correctly defined or other appropriate information about the statistical significance of the experiments?

Answer: [No]

Justification: Training language models is expensive, hence we cannot afford to train with multiple seeds to provide error bars on the performance. We report the mean and standard deviation of the latency and throughput of all methods in the appendix.

Guidelines:

- The answer NA means that the paper does not include experiments.
- The authors should answer "Yes" if the results are accompanied by error bars, confidence intervals, or statistical significance tests, at least for the experiments that support the main claims of the paper.
- The factors of variability that the error bars are capturing should be clearly stated (for example, train/test split, initialization, random drawing of some parameter, or overall run with given experimental conditions).
- The method for calculating the error bars should be explained (closed form formula, call to a library function, bootstrap, etc.)
- The assumptions made should be given (e.g., Normally distributed errors).
- It should be clear whether the error bar is the standard deviation or the standard error of the mean.
- It is OK to report 1-sigma error bars, but one should state it. The authors should preferably report a 2-sigma error bar than state that they have a 96% CI, if the hypothesis of Normality of errors is not verified.
- For asymmetric distributions, the authors should be careful not to show in tables or figures symmetric error bars that would yield results that are out of range (e.g. negative error rates).
- If error bars are reported in tables or plots, The authors should explain in the text how they were calculated and reference the corresponding figures or tables in the text.

8. Experiments compute resources

Question: For each experiment, does the paper provide sufficient information on the computer resources (type of compute workers, memory, time of execution) needed to reproduce the experiments?

Answer: [Yes]

Justification: We provide details on the training and inference compute resources in Appendix A

Guidelines:

- The answer NA means that the paper does not include experiments.
- The paper should indicate the type of compute workers CPU or GPU, internal cluster, or cloud provider, including relevant memory and storage.
- The paper should provide the amount of compute required for each of the individual experimental runs as well as estimate the total compute.
- The paper should disclose whether the full research project required more compute than the experiments reported in the paper (e.g., preliminary or failed experiments that didn't make it into the paper).

9. Code of ethics

Question: Does the research conducted in the paper conform, in every respect, with the NeurIPS Code of Ethics <https://neurips.cc/public/EthicsGuidelines>?

Answer: [Yes]

Justification: Our research does not involve human subjects or participants. The datasets are well established and widely used by prior work. While the data might contain certain biases, as it originates from the internet, our models are small (<300M parameters) compared to state-of-the-art models, hence we do not believe that an ill-intentioned user would be using them to cause harm, while much stronger alternative models exist.

Guidelines:

- The answer NA means that the authors have not reviewed the NeurIPS Code of Ethics.
- If the authors answer No, they should explain the special circumstances that require a deviation from the Code of Ethics.
- The authors should make sure to preserve anonymity (e.g., if there is a special consideration due to laws or regulations in their jurisdiction).

10. Broader impacts

Question: Does the paper discuss both potential positive societal impacts and negative societal impacts of the work performed?

Answer: [Yes]

Justification: We discuss the societal impacts of our work here. Language models are dual-use technologies, and thus, they can have unethical uses, such as fake content generation, and they can suffer from bias if applied to data sets that are not carefully curated. This paper focuses specifically on speeding up discrete diffusion language models at test time to reduce their computational demands; while the performance of our PGMs improves over MDLMs, it remains unclear whether diffusion language models can overtake large autoregressive models at scale, hence we do not have specific concerns with regard to this contribution.

Guidelines:

- The answer NA means that there is no societal impact of the work performed.
- If the authors answer NA or No, they should explain why their work has no societal impact or why the paper does not address societal impact.
- Examples of negative societal impacts include potential malicious or unintended uses (e.g., disinformation, generating fake profiles, surveillance), fairness considerations (e.g., deployment of technologies that could make decisions that unfairly impact specific groups), privacy considerations, and security considerations.
- The conference expects that many papers will be foundational research and not tied to particular applications, let alone deployments. However, if there is a direct path to any negative applications, the authors should point it out. For example, it is legitimate to point out that an improvement in the quality of generative models could be used to generate deepfakes for disinformation. On the other hand, it is not needed to point out that a generic algorithm for optimizing neural networks could enable people to train models that generate Deepfakes faster.

- The authors should consider possible harms that could arise when the technology is being used as intended and functioning correctly, harms that could arise when the technology is being used as intended but gives incorrect results, and harms following from (intentional or unintentional) misuse of the technology.
- If there are negative societal impacts, the authors could also discuss possible mitigation strategies (e.g., gated release of models, providing defenses in addition to attacks, mechanisms for monitoring misuse, mechanisms to monitor how a system learns from feedback over time, improving the efficiency and accessibility of ML).

11. Safeguards

Question: Does the paper describe safeguards that have been put in place for responsible release of data or models that have a high risk for misuse (e.g., pretrained language models, image generators, or scraped datasets)?

Answer: [No]

Justification: We did not introduce any safeguards such as alignment of our models since they have less than 300M parameters. We expect ill-intentioned users to prefer state-of-the-art, instruction tuned models for nefarious deeds, hence it did not appear necessary to align our models.

Guidelines:

- The answer NA means that the paper poses no such risks.
- Released models that have a high risk for misuse or dual-use should be released with necessary safeguards to allow for controlled use of the model, for example by requiring that users adhere to usage guidelines or restrictions to access the model or implementing safety filters.
- Datasets that have been scraped from the Internet could pose safety risks. The authors should describe how they avoided releasing unsafe images.
- We recognize that providing effective safeguards is challenging, and many papers do not require this, but we encourage authors to take this into account and make a best faith effort.

12. Licenses for existing assets

Question: Are the creators or original owners of assets (e.g., code, data, models), used in the paper, properly credited and are the license and terms of use explicitly mentioned and properly respected?

Answer: [Yes]

Justification: The licenses for the datasets are discussed in Appendix A, and we cite the original work that introduced the datasets and models that we use.

Guidelines:

- The answer NA means that the paper does not use existing assets.
- The authors should cite the original paper that produced the code package or dataset.
- The authors should state which version of the asset is used and, if possible, include a URL.
- The name of the license (e.g., CC-BY 4.0) should be included for each asset.
- For scraped data from a particular source (e.g., website), the copyright and terms of service of that source should be provided.
- If assets are released, the license, copyright information, and terms of use in the package should be provided. For popular datasets, paperswithcode.com/datasets has curated licenses for some datasets. Their licensing guide can help determine the license of a dataset.
- For existing datasets that are re-packaged, both the original license and the license of the derived asset (if it has changed) should be provided.
- If this information is not available online, the authors are encouraged to reach out to the asset's creators.

13. New assets

Question: Are new assets introduced in the paper well documented and is the documentation provided alongside the assets?

Answer: [Yes]

Justification: Appendix A presents all hyperparameters. We provide our training code in the supplementary material, along with commands to reproduce our results.

Guidelines:

- The answer NA means that the paper does not release new assets.
- Researchers should communicate the details of the dataset/code/model as part of their submissions via structured templates. This includes details about training, license, limitations, etc.
- The paper should discuss whether and how consent was obtained from people whose asset is used.
- At submission time, remember to anonymize your assets (if applicable). You can either create an anonymized URL or include an anonymized zip file.

14. Crowdsourcing and research with human subjects

Question: For crowdsourcing experiments and research with human subjects, does the paper include the full text of instructions given to participants and screenshots, if applicable, as well as details about compensation (if any)?

Answer: [NA]

Justification: We do not perform experiments with human subjects.

Guidelines:

- The answer NA means that the paper does not involve crowdsourcing nor research with human subjects.
- Including this information in the supplemental material is fine, but if the main contribution of the paper involves human subjects, then as much detail as possible should be included in the main paper.
- According to the NeurIPS Code of Ethics, workers involved in data collection, curation, or other labor should be paid at least the minimum wage in the country of the data collector.

15. Institutional review board (IRB) approvals or equivalent for research with human subjects

Question: Does the paper describe potential risks incurred by study participants, whether such risks were disclosed to the subjects, and whether Institutional Review Board (IRB) approvals (or an equivalent approval/review based on the requirements of your country or institution) were obtained?

Answer: [NA]

Justification: We do not perform experiments with human subjects.

Guidelines:

- The answer NA means that the paper does not involve crowdsourcing nor research with human subjects.
- Depending on the country in which research is conducted, IRB approval (or equivalent) may be required for any human subjects research. If you obtained IRB approval, you should clearly state this in the paper.
- We recognize that the procedures for this may vary significantly between institutions and locations, and we expect authors to adhere to the NeurIPS Code of Ethics and the guidelines for their institution.
- For initial submissions, do not include any information that would break anonymity (if applicable), such as the institution conducting the review.

16. Declaration of LLM usage

Question: Does the paper describe the usage of LLMs if it is an important, original, or non-standard component of the core methods in this research? Note that if the LLM is used only for writing, editing, or formatting purposes and does not impact the core methodology, scientific rigor, or originality of the research, declaration is not required.

Answer: [NA]

Justification: We have not used LLMs to derive components of this work. We had a light use of an LLM to rephrase a few sentences and find synonyms.

Guidelines:

- The answer NA means that the core method development in this research does not involve LLMs as any important, original, or non-standard components.
- Please refer to our LLM policy (<https://neurips.cc/Conferences/2025/LLM>) for what should or should not be described.

Table 6: Sample quality and efficiency of PGM 6 / 6 (dim. 1024) with uniform sampling on OpenWebText with different numbers of sampling steps *after distillation with SDTT*. We generate sequences of 1024 tokens with a batch size of 32 to measure the latency and throughput. See Table 5 for un-distilled models. Observe that distillation using FP64 preserves the entropy better than distillation in FP32.

| Model | Gen. PPL ↓ | Entropy ↑ | Latency ↓ (ms) | Throughput ↑ (tok/s) |
|---|-------------------|------------------|---------------------------|---------------------------------|
| <i>PGM 6 / 6 (dim. 1024, uniform sampling)</i> | | | | |
| 32 steps | 185.16 | 5.73 | 1.59 ± 0.01 | 20'569.99 ± 95.63 |
| 64 steps | 138.87 | 5.70 | 3.03 ± 0.01 | 10'805.31 ± 14.11 |
| 128 steps | 116.95 | 5.67 | 5.93 ± 0.01 | 5'518.09 ± 13.46 |
| 256 steps | 108.51 | 5.65 | 11.77 ± 0.01 | 2'782.78 ± 3.46 |
| 512 steps | 101.94 | 5.63 | 23.25 ± 0.01 | 1'408.88 ± 1.05 |
| 1024 steps | 99.64 | 5.62 | 46.31 ± 0.02 | 707.52 ± 0.34 |
| <i>+ SDTT (10k steps per round, loss in FP32, 7 rounds)</i> | | | | |
| 8 steps | 176.62 | 5.48 | 0.51 ± 0.00 | 63'342.23 ± 206.49 |
| 16 steps | 100.50 | 5.44 | 0.87 ± 0.00 | 37'607.96 ± 49.61 |
| 32 steps | 72.19 | 5.40 | 1.59 ± 0.01 | 20'569.99 ± 95.63 |
| 64 steps | 59.59 | 5.35 | 3.03 ± 0.01 | 10'805.31 ± 14.11 |
| 128 steps | 55.44 | 5.31 | 5.93 ± 0.01 | 5'518.09 ± 13.46 |
| 256 steps | 50.80 | 5.29 | 11.77 ± 0.01 | 2'782.78 ± 3.46 |
| 512 steps | 49.72 | 5.27 | 23.25 ± 0.01 | 1'408.88 ± 1.05 |
| 1024 steps | 49.48 | 5.28 | 46.31 ± 0.02 | 707.52 ± 0.34 |
| <i>+ SDTT (10k steps per round, loss in FP32, 5 rounds)</i> | | | | |
| 8 steps | 268.81 | 5.62 | 0.51 ± 0.00 | 63'342.23 ± 206.49 |
| 16 steps | 140.89 | 5.59 | 0.87 ± 0.00 | 37'607.96 ± 49.61 |
| 32 steps | 92.06 | 5.54 | 1.59 ± 0.01 | 20'569.99 ± 95.63 |
| 64 steps | 73.94 | 5.50 | 3.03 ± 0.01 | 10'805.31 ± 14.11 |
| 128 steps | 64.45 | 5.47 | 5.93 ± 0.01 | 5'518.09 ± 13.46 |
| 256 steps | 60.70 | 5.46 | 11.77 ± 0.01 | 2'782.78 ± 3.46 |
| 512 steps | 57.94 | 5.44 | 23.25 ± 0.01 | 1'408.88 ± 1.05 |
| 1024 steps | 57.26 | 5.43 | 46.31 ± 0.02 | 707.52 ± 0.34 |
| <i>+ SDTT (10k steps per round, loss in FP64, 7 rounds)</i> | | | | |
| 8 steps | 223.52 | 5.57 | 0.51 ± 0.00 | 63'342.23 ± 206.49 |
| 16 steps | 124.70 | 5.54 | 0.87 ± 0.00 | 37'607.96 ± 49.61 |
| 32 steps | 86.64 | 5.49 | 1.59 ± 0.01 | 20'569.99 ± 95.63 |
| 64 steps | 71.93 | 5.46 | 3.03 ± 0.01 | 10'805.31 ± 14.11 |
| 128 steps | 63.35 | 5.43 | 5.93 ± 0.01 | 5'518.09 ± 13.46 |
| 256 steps | 60.44 | 5.42 | 11.77 ± 0.01 | 2'782.78 ± 3.46 |
| 512 steps | 58.29 | 5.40 | 23.25 ± 0.01 | 1'408.88 ± 1.05 |
| 1024 steps | 58.33 | 5.41 | 46.31 ± 0.02 | 707.52 ± 0.34 |
| <i>+ SDTT (10k steps per round, loss in FP64, 5 rounds)</i> | | | | |
| 8 steps | 289.35 | 5.66 | 0.51 ± 0.00 | 63'342.23 ± 206.49 |
| 16 steps | 152.81 | 5.63 | 0.87 ± 0.00 | 37'607.96 ± 49.61 |
| 32 steps | 101.61 | 5.59 | 1.59 ± 0.01 | 20'569.99 ± 95.63 |
| 64 steps | 82.73 | 5.56 | 3.03 ± 0.01 | 10'805.31 ± 14.11 |
| 128 steps | 70.36 | 5.53 | 5.93 ± 0.01 | 5'518.09 ± 13.46 |
| 256 steps | 68.23 | 5.53 | 11.77 ± 0.01 | 2'782.78 ± 3.46 |
| 512 steps | 65.69 | 5.51 | 23.25 ± 0.01 | 1'408.88 ± 1.05 |
| 1024 steps | 64.22 | 5.50 | 46.31 ± 0.02 | 707.52 ± 0.34 |

Table 7: Sample quality and efficiency *after distillation* of PGM 6 / 6 (dim. 1024) and MDLM. We generate sequences of 1024 tokens with a batch size of 32 to measure the latency and throughput. See Table 5 for un-distilled models. SDTT is more effective at reducing the Generative perplexity of MDLMs, although the Entropy of MDLM+SDTT is more severely reduced compared to PGM+SDTT.

| Model | Gen. PPL ↓ | Entropy ↑ | Latency ↓ (ms) | Throughput ↑ (tok/s) |
|--|-------------------|------------------|---------------------------|---------------------------------|
| <i>PGM+SDTT (10k steps per round, loss in FP32, 7 rounds)</i> | | | | |
| 32 steps | 72.19 | 5.40 | 1.59 ± 0.01 | 20'569.99 ± 95.63 |
| 64 steps | 59.59 | 5.35 | 3.03 ± 0.01 | 10'805.31 ± 14.11 |
| 128 steps | 55.44 | 5.31 | 5.93 ± 0.01 | 5'518.09 ± 13.46 |
| 256 steps | 50.80 | 5.29 | 11.77 ± 0.01 | 2'782.78 ± 3.46 |
| 512 steps | 49.72 | 5.27 | 23.25 ± 0.01 | 1'408.88 ± 1.05 |
| 1024 steps | 49.48 | 5.28 | 46.31 ± 0.02 | 707.52 ± 0.34 |
| <i>MDLM+SDTT (10k steps per round, loss in FP32, 7 rounds)</i> | | | | |
| 32 steps | 56.34 | 5.27 | 8.037 ± 0.01 | 4'077.08 ± 3.06 |
| 64 steps | 46.45 | 5.22 | 15.82 ± 0.01 | 2'070.67 ± 0.69 |
| 128 steps | 40.61 | 5.18 | 31.41 ± 0.01 | 1'043.22 ± 0.16 |
| 256 steps | 38.92 | 5.15 | 62.54 ± 0.01 | 523.90 ± 0.06 |
| 512 steps | 37.35 | 5.14 | 124.94 ± 0.16 | 262.26 ± 0.33 |
| 1024 steps | 36.08 | 5.11 | 249.31 ± 0.11 | 131.42 ± 0.05 |

Table 8: Sample quality and efficiency on ImageNet with different numbers of sampling steps. As shown in Figure 4, in situations where the inference cost is limited, PGM outperforms MDLM. Our goal is not to reach the state-of-the-art, since we train relatively smaller models with the exact same configurations as for experiments on text, for simplicity. Optimizing PGMs for images is left to future work.

| Model | FID ↓ | IS ↑ | Latency ↓ (ms) | Throughput ↑ (tok/s) |
|---|--------------|-------------|---------------------------|---------------------------------|
| <i>MDLM</i> | | | | |
| 8 steps | 98.43 | 12.22 | 2.49 ± 0.01 | 26'331.16 ± 23.77 |
| 16 steps | 81.80 | 14.87 | 4.72 ± 0.01 | 13'918.07 ± 4.57 |
| 32 steps | 71.13 | 16.33 | 9.18 ± 0.01 | 7'164.60 ± 2.93 |
| 64 steps | 67.07 | 17.13 | 18.09 ± 0.01 | 3'635.35 ± 1.09 |
| 128 steps | 62.50 | 18.49 | 35.91 ± 0.01 | 1'831.69 ± 0.44 |
| 256 steps | 54.47 | 19.40 | 71.56 ± 0.02 | 919.31 ± 0.26 |
| <i>PGM 8 / 4 (dim. 1024, non-uniform)</i> | | | | |
| 8 steps | 102.34 | 11.56 | 1.70 ± 0.01 | 3'635.70 ± 421.41 |
| 16 steps | 85.22 | 13.92 | 3.02 ± 0.02 | 21'725.97 ± 188.56 |
| 32 steps | 74.69 | 16.06 | 5.65 ± 0.03 | 11'641.26 ± 67.16 |
| 64 steps | 68.48 | 17.54 | 10.83 ± 0.10 | 6'070.08 ± 59.86 |
| 128 steps | 65.83 | 18.71 | 20.46 ± 0.23 | 3'215.10 ± 35.89 |
| 256 steps | 63.44 | 18.52 | 37.71 ± 0.52 | 1'744.82 ± 24.00 |
| <i>PGM 8 / 4 (dim. 1024, uniform)</i> | | | | |
| 8 steps | 100.54 | 11.88 | 0.82 ± 0.00 | 79'838.18 ± 65.09 |
| 16 steps | 84.42 | 14.44 | 1.54 ± 0.01 | 42'483.88 ± 49.88 |
| 32 steps | 73.69 | 16.41 | 2.98 ± 0.01 | 22'006.84 ± 26.18 |
| 64 steps | 66.00 | 17.66 | 5.90 ± 0.01 | 11'148.64 ± 8.70 |
| 128 steps | 64.45 | 17.98 | 11.71 ± 0.01 | 5'615.94 ± 2.75 |
| 256 steps | 61.37 | 19.09 | 23.33 ± 0.01 | 2'819.38 ± 0.58 |